Frontiers in Heat and Mass Transfer (FHMT), 20, 14 (2023)
DOI: 10.5098/hmt.20.14

Global Digital Central
ISSN: 2151-8629

Frontiers in Heat and Mass Transfer

Available at www.ThermalFluidsCentral.org

NUMERICAL SIMULATION ON HEAT TRANSFER OF MULTI-LAYER LADLE IN EMPTY AND HEAVY CONDITION

Linfang Fang, Fuyong Su*, Zhen Kang, Haojun Zhu

School of Energy and Environmental Engineering, University of Science and Technology Beijing, Beijing,100083, China

ABSTRACT

Taking the ladle used by a factory as an example, a three-dimensional finite element model of the ladle was established, and the temperature distribution law of the lining during the ladle transportation was studied using the finite element analysis software ANSYS, which verified the good thermal insulation performance of the nano thermal insulation layer, and analyzed and compared the temperature and distribution law of the refractory lining under the two working conditions of the heavy ladle and the empty ladle. The results show that due to the change of the boundary conditions in the empty ladle state, the temperature change trend of the working layer and slag line layer along the thickness direction changes, but the overall temperature distribution of other layers does not change much; The temperature of the inner liner generally tends to be high inside and low outside, with a large temperature gradient along the radial direction. Therefore, during the production process, it is necessary to try to avoid sharp changes in the temperature of the inner liner, and regularly maintain the refractory materials to extend the service life of the ladle.

Keywords: *Ladle，Refractory，Heavy ladle，Empty ladle，Temperature field*

1. INTRODUCTION

The ladle is a high-temperature container that directly stores molten steel between steelmaking and continuous casting, and is an important equipment in the steelmaking process. In the process of ladle thermal cycle, the iron and steel smelting process are long, the process is numerous, the process cycle is long, the time-consuming changes are large, and there are many uncertain factors. Moreover, during the use of the ladle, it not only has to bear the effects of mechanical loads such as its own weight and the gravity of the molten steel, but also bear the influence of the high temperature thermal load of the molten steel. The load conditions are complex and the working environment is harsh. Due to periodic flame baking, erosion and erosion of molten steel, the refractory lining will continue to crack and corrode.

In the past, some scholars have studied the damage causes of ladle refractories and cladding, and the results show that the damage of ladle refractories has a great relationship with its thermo-mechanical stress (Kondrukevich and Ryabyi, 2018; Schmitt et al., 2004; Ning et al., 2019; Ryabyi et al., 2017). The damage caused by high temperature gradient is an important cause of thermal mechanical damage of lining refractory (Gruber and Harmuth, 2014). Therefore, it is of great significance to study the temperature field distribution and temperature change during ladle turnover to optimize the technological process, improve the steel-making quality, extend the service life of ladle and ensure production safety.

To study the temperature field, it is first necessary to analyze the corresponding heat transfer processes, including convective and radiant heat transfer processes. Previously, some scholars have studied the radiation and convective heat transfer processes of some thermal equipment (Wahlquist et al., 2022; Prasad et al., 2022). Zabolotsky (2011) proposed a method for calculating the temperature field of the casting ladle lining by a modified relaxation method. Given such initial data as the metal temperature in the ladle, the ambient temperature, and the lining structure, this method permits calculating the stationary temperature fields both inside the lining and on the surface of the ladle jacket.

Volkova and Janke (2003) carried out mathematical modeling of heat transfer in ladle based on Fourier differential equation, and established a numerical model of ladle temperature field considering heat transfer factors, which can be used to predict the temperature field of ladle in different casting processes. Cheng et al. (2015) used the finite element analysis software ANSYS and the indirect coupling method to calculate, and obtained the temperature change and stress distribution of the lining when the ladle was filled with steel under different baking and preheating temperature conditions. Li (2015) analyzed the temperature field and stress field of the new type of ladle with the nanometer adiabatic material in lining structure after baking. Farrera-Buenrostro et al. (2019) simulated the radiation of the free surface of the ladle and compared the thermal behavior of magnesium carbon (MgO-C) and high alumina (Al_2O_3) commonly used in industry as working liners. Sun et al. (2020) used steady-state analysis and numerical simulation techniques to compare and analyze the temperature distribution of the new lightweight ladle and the traditional ladle under typical operation modes. Qiu et al. (2022) studied the influence of ladle cover and liquid level on the temperature drop rate during the standing temperature drop of 210 t ladle.

In this paper, the temperature field under two working conditions of heavy ladle and empty ladle are studied by using the finite element analysis software ANSYS. The temperature distribution of the ladle under the two conditions is calculated, and the temperature distribution law is analyzed.

*Corresponding author. Email: sfyong@ustb.edu.cn

Global Digital Central
ISSN: 2151-8629

2. MATHEMATICAL MODEL AND FINITE ELEMENT MODEL

2.1 Ladle Lining Structure

The ladle is mainly composed of a ladle shell and a ladle lining cast by a refractory lining; The ladle shell is composed of ladle bottom, ladle wall, trunnion and support. The ladle lining is composed of slag line layer, working layer, permanent layer and nano thermal insulation layer. The ladle lining structure is shown in Figure 1.

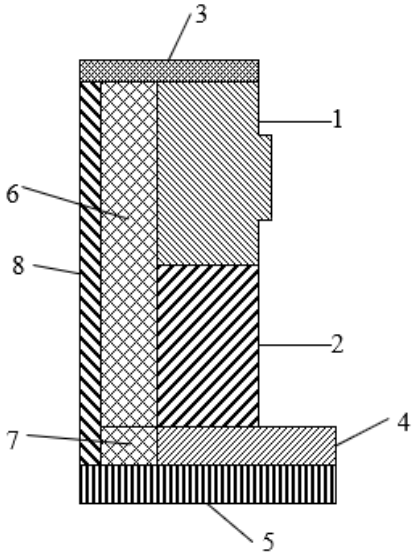

1- Slag line layer；2- Wall working layer；3-Ladle edge；
4- Bottom working layer；5- Bottom permanent layer；
6- Wall permanent layer；
7- Outer permanent layer of the bottom working layer；
8- Nano thermal insulation layer

Fig. 1 Schematic diagram of ladle lining structure

The materials and main dimensions of the ladle lining are shown in Table 1.

Table 1 Materials and Thickness of lining layer

Position	*Refractory layer*	*Material*	*Thickness* (mm)
Ladle wall	Slag line layer	MgO-C Bricks	210/230
	Working layer	High purity alumina magnesia castable	200
	Permanent layer	High alumina castable	90
	Nano thermal insulation layer	Nano thermal insulation board	8
	Shell	--	32
Ladle bottom	Working layer	High purity alumina magnesia castable	350
	Permanent layer	High alumina castable	100
	Shell	--	60

2.2 Establishment of Finite Element Model

According to the structure and size of the ladle, the ladle is modeled. During the modeling process, the structures such as the breathable bricks at the bottom of the ladle and the sliding nozzle plate are ignored. The established physical model is shown in Figure 2.

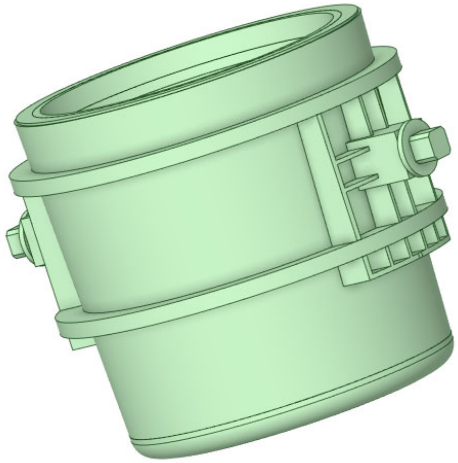

Fig. 2 Physical model of ladle

It can be seen that the ladle model is a symmetrical structure. In order to save computational resources, half of the ladle is taken as the finite element analysis object. In order to ensure high grid quality, the ladle is divided into blocks and more complex parts are densified during grid division.

The model after grid division is shown in Figure 3.

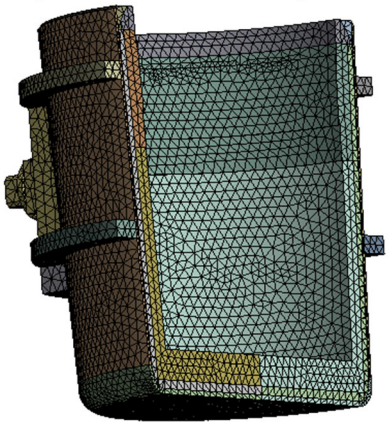

Fig. 3 Finite element model of ladle

2.3 Mathematical Model of Heat Transfer

The mass conservation equation, momentum conservation equation and energy conservation equation (Bhagat and Deshmukh, 2021) in the research process are as follows：

(1) Continuity equation

$$\frac{\partial \rho}{\partial t} + div(\rho \vec{v}) = 0 \quad (1)$$

(2) Momentum conservation equation:

$$\frac{\partial \vec{v}}{\partial t} + (\vec{v} \cdot \nabla)\vec{v} = \vec{f} - \frac{1}{\rho} gradp + \upsilon \nabla^2 \vec{v} \quad (2)$$

Where ρ is the fluid density (kg/m^3); t is the time; $\vec{v} = [v_x v_y v_z]^T$,and v_x, $v_y$and v_z respectively represent the velocity along the directions of x, y, and z (m/s); $\vec{f} = [f_x f_y f_z]^T$,and f_x, f_y and f_z respectively

Global Digital Central
ISSN: 2151-8629

represent the mass power along the directions of x, y, and z; p represent the liquid pressure (Pa); υ is the kinematic viscosity of fluid(m^2/s).

(3) Energy conservation equation:

$$\frac{\partial \rho T}{\partial t} + div(\rho \vec{v} T) = div\left(\frac{\lambda}{C_p} gradT\right) + S_T \quad (3)$$

Where T is the temperature(K), λ is the thermal conductivity of fluid(W/(m·K)); C_p is the is the specific heat capacity(J/kg·K); $S_T = S_h + \Phi$, S_T is the source item, S_h and Φ are, respectively, the heat source and dissipation function.

2.4 Mesh Independence Verification

Verify the grid independence of the ladle temperature field, select the axial temperature change of the permanent layer as the judgment basis of grid independence, select four grid drawing schemes, and the number of grids is 71750, 111839, 202873 and 435363 respectively. The temperature difference obtained in schemes 2, 3 and 4 is no more than 2K at most. It can be considered that these schemes have sufficient calculation accuracy. At the same time, considering the capacity of the computer, the mesh size with the mesh number of 202873 is taken for simulation calculation. The grid independence verification results are shown in Figure 4.

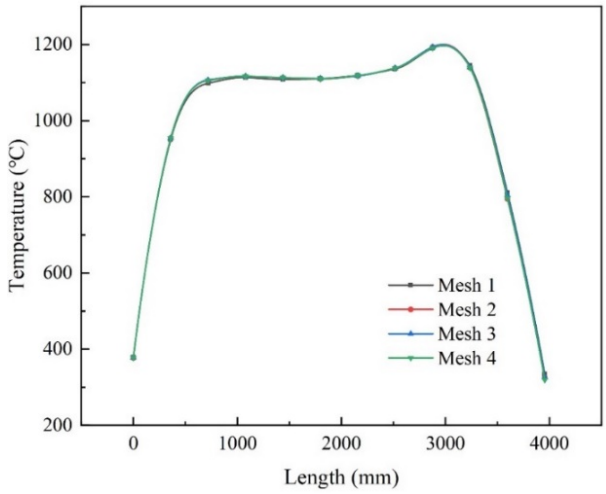

Fig. 4 Grid independence verification

2.5 Boundary Conditions, Initial Conditions and Physical Parameters

The inner lining of the working layer is in contact with the molten steel in the heavy ladle state; In the empty ladle state, the inner lining of the working layer and the surrounding environment conduct radiation and convection heat exchange; During the thermal cycle of the outer surface of the ladle lining, its heat dissipation mainly includes two paths, one is the natural convection heat exchange with the air, and the other is the radiation heat exchange between the ladle and the surrounding. In the calculation, the comprehensive convection heat transfer coefficient is taken as $12.07\,W\cdot\left(m^2\cdot K\right)^{-1}$, the ambient temperature is taken as 30 ℃, and the molten steel temperature is set as 1450 ℃.

In the calculation process, the steady-state thermal analysis of the ladle is carried out first, and then the results of the steady-state thermal analysis are taken as the initial conditions for the transient analysis.

The physical parameters of inner lining layer of the ladle are shown in Table 2.

Table 2 Physical parameters of each inner lining material of ladle

Layer	*Coefficient of thermal conductivity* (W/(m·K))	*Specific heat capacity* (J/Kg·K)	*Density* ($Kg\cdot m^{-3}$)	*Blackness*
Ladle edge	0.9	1150	2600	--
Slag line layer	2.525	1130	2900	--
Working layer	1.6	1255	3050	--
Permanent layer	0.9	1090	2600	--
Nano thermal insulation layer	0.034	613	560	--
Shell	42	816	7800	--
Steel	40.3	750	7200	0.65

3. ANALYSIS OF LADEL TEMPERATURE FIELD

The simulation calculation was performed in Ansys. The molten steel temperature was set at 1450°C, the convection boundary conditions were set on the outer surface of the ladle, the comprehensive convection heat transfer coefficient was taken as $12.07\,W\cdot\left(m^2\cdot K\right)^{-1}$, and the ambient temperature was taken as 30 ℃. The cloud diagram of steady-state temperature distribution of the ladle is calculated, as shown in Figure 5.

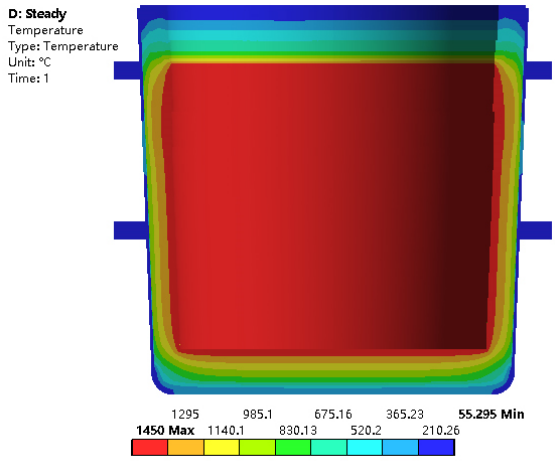

Fig. 5 Temperature distribution of ladle section under steady state

The temperature distribution of each refractory layer in this stable state is shown in Table 3.

Table 3 Temperature distribution of refractory layer

Layer	*Average temperature* (℃)	*Maximum temperature* (℃)	*Minimum temperature* (℃)
Working layer	1160	1450	375
Slag line layer	1183	1450	331
Permanent layer	757	1194	143
Nano thermal insulation layer	465	906	102
Shell	153	286	55

The results show that the temperature of the inner lining decreases sequentially from the inside to the outside. The working layer and the slag line layer are in direct contact with the molten steel, and the temperature is higher, with an average temperature of about 1160℃ and 1183℃; the permanent layer and the nano thermal insulation layer have the highest temperature. The temperatures are 1194℃ and 906℃ respectively, which are significantly lower than those of the inner liner directly in contact with molten steel; due to the excellent thermal insulation performance of the nano thermal insulation layer, the ladle shell temperature is maintained in a low range, with an average temperature of 153℃.

3.1 Temperature Field Analysis of Heavy Ladle in Static State

The temperature distribution of the lining in the stable state was taken as the initial condition to conduct transient analysis, and the ladle temperature in the static state of heavy ladle was studied. After natural cooling for 2 hours, the temperature distribution cloud diagram of the ladle section in the state of heavy ladle is shown in Figure 6.

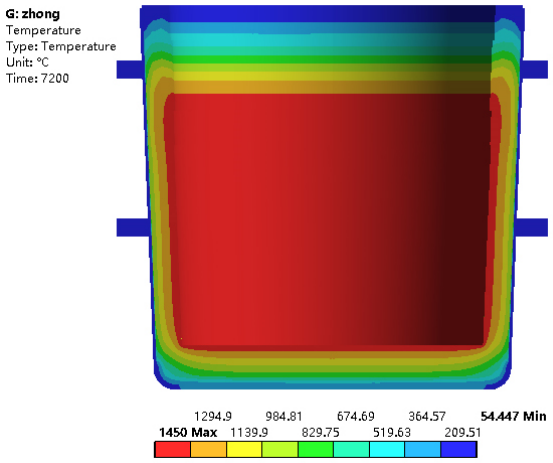

Fig. 6 Temperature distribution of ladle cross-section after heavy ladle rest for 2 hours

The temperature distribution of each refractory layer in heavy ladle state is shown in Table 4.

Table 4 Temperature distribution of refractory layer

Layer	*Average temperature* (℃)	*Maximum temperature* (℃)	*Minimum temperature* (℃)
Working layer	1155	1433	373
Slag line layer	1083	1430	316
Permanent layer	755	1193	142
Nano thermal insulation layer	461	905	100
Shell	149	280	54

The temperature distribution of each inner lining layer of the ladle in this state is shown in Figure 7.

(a)

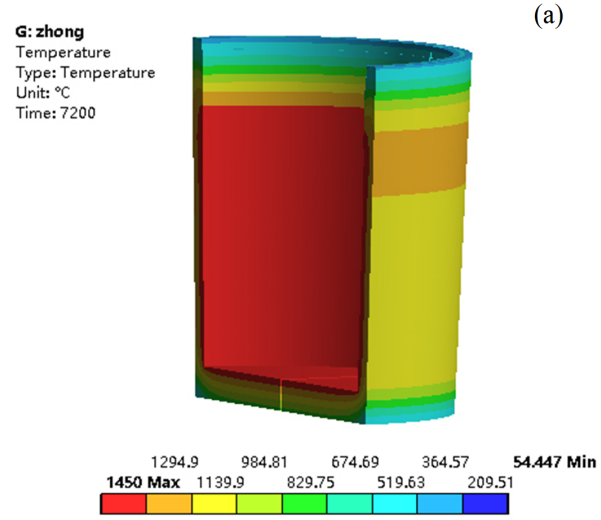

(a) Working layer

(b)

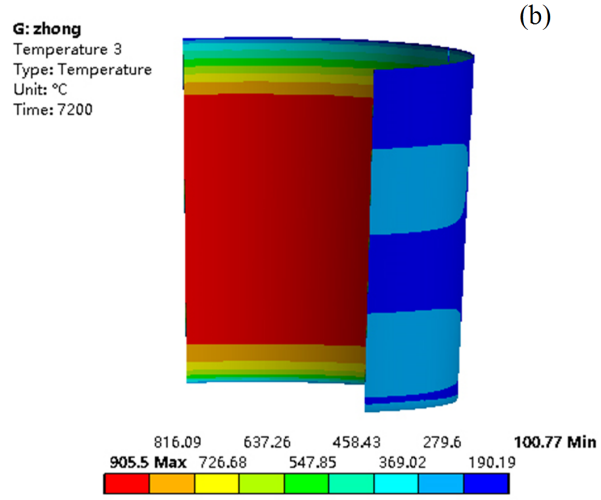

(b) Nano thermal insulation layer

(c)

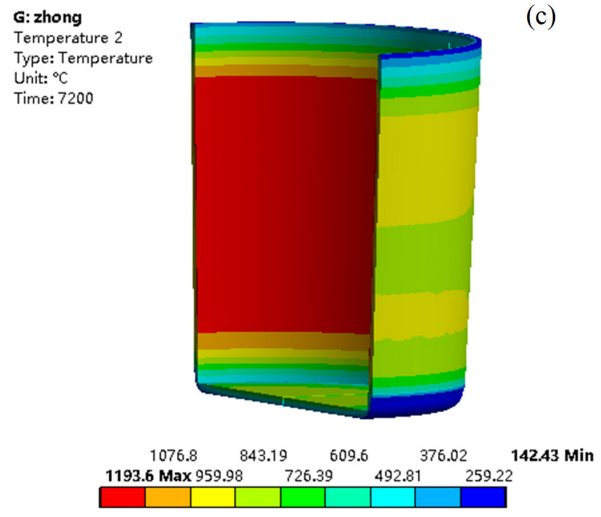

(c) Permanent layer

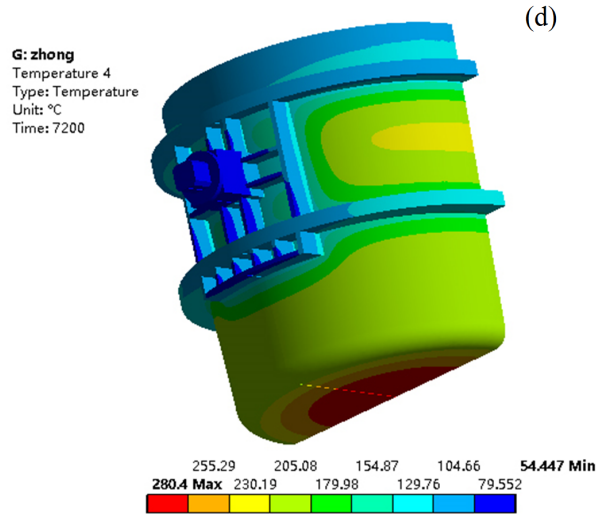

(d) Ladle shell

Fig. 7 Temperature distribution of each inner lining layer of the ladle in the static state of heavy ladle

It can be seen from the analysis results that the average temperature of each inner lining layer of the ladle decreases compared with the steady state after the steel is placed for 2 hours. The temperature changes of the working layer and the slag line layer along the thickness direction are shown in Figure 8. Since the inner lining layer is still in contact with molten steel, the temperature is relatively high. The average temperature is about 1155°C and 1083°C, respectively. The part where the inner lining is in contact with the molten steel, and the temperature gradually decreases from the inside to the outside. Because of the thicker thickness of the bottom working layer, the temperature is lower than that of the outside of the wall;

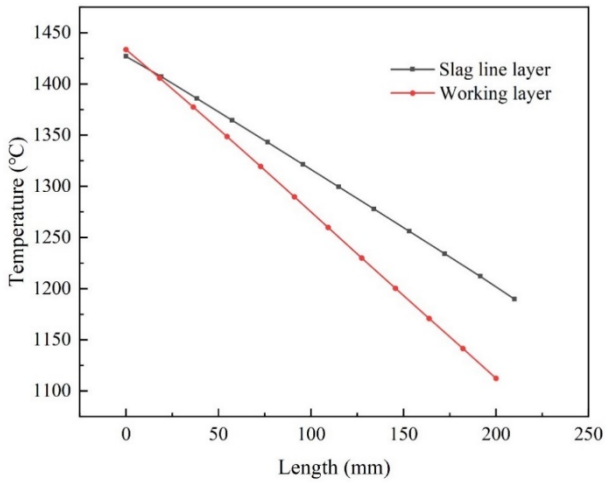

Fig. 8 Temperature change of working layer and slag line layer wall in thickness direction

The temperature variation of the permanent layer along the thickness direction is shown in Figure 9. The average temperature of the layer is maintained at about 755 ℃, and the maximum temperature is 1193 ℃, which appears at the position where the inner side contacts the working layer, and the temperature distribution also shows a trend of low outside and high inside;

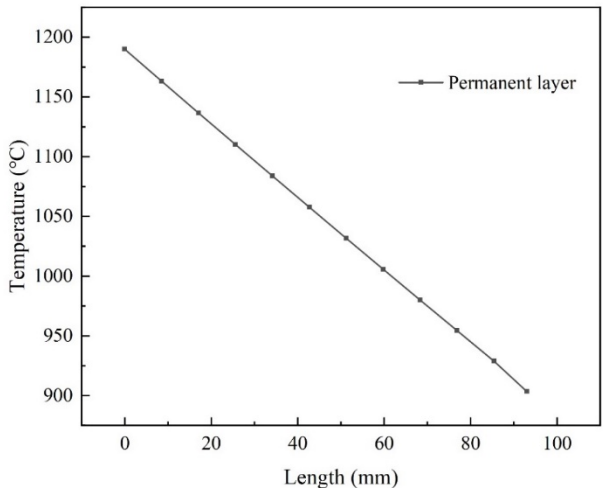

Fig. 9 Temperature change in the thickness direction of the permanent layer

The temperature variation of the nano thermal insulation layer along the thickness direction is shown in Figure 10. The average temperature of the layer is maintained at about 461 ℃, and the temperature variation trend along the thickness direction is similar to that of other linings, but the temperature gradient is large. The maximum temperature on the inner side reaches 905 ℃, while the minimum temperature on the outside is only 209 ℃, and the temperature difference between the inner and outer surfaces is 696 ℃, which indicates that the nano thermal insulation layer has good thermal insulation performance. It can reduce the heat loss of ladle to a great extent.

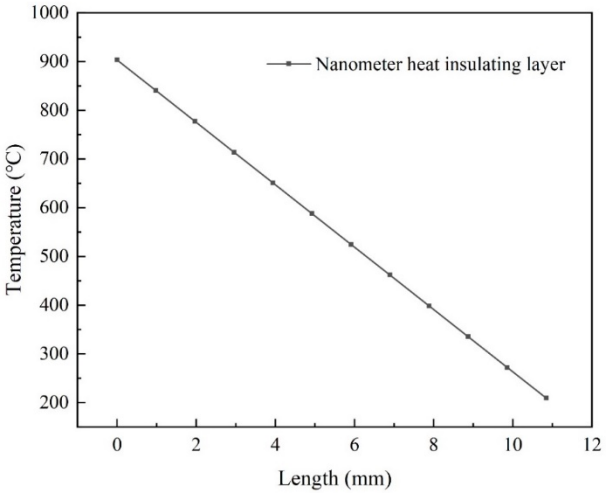

Fig. 10 Temperature change in the thickness direction of the Nano thermal insulation layer

The temperature change of the inner and outer walls of the ladle shell axis is shown in Figure 11. The average temperature of the ladle shell is 149 ℃, and the overall temperature on the inner side of the ladle shell is slightly higher than that on the outer side when holding steel. The maximum temperature is 280 ℃, which appears at the bottom of the ladle. This is because there is no nano thermal insulation layer at the

bottom of the ladle as the thermal insulation layer, resulting in large heat transfer from the bottom to the outside, and the minimum temperature is 54 ℃, which appears at the trunnion of the ladle.

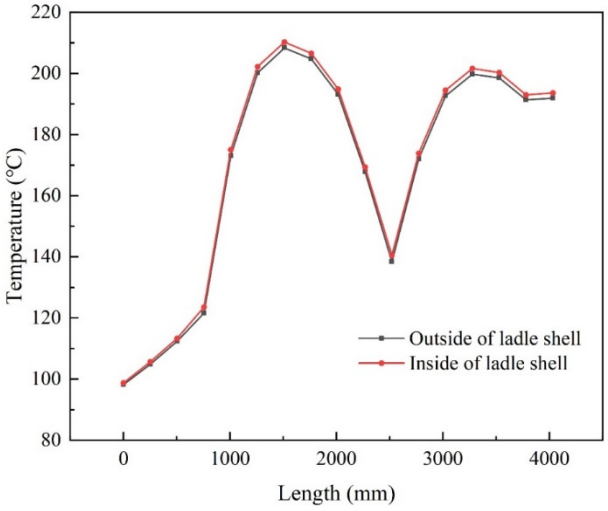

Fig. 11 Temperature change of inner and outer walls of ladle shell in axial direction

From the above analysis, it can be seen that the temperature distribution of each inner lining layer of the ladle shows a trend of low outside and high inside, and the parts with lower temperature of each layer are mainly concentrated at the trunnion of the ladle and the edge of the bottom of the ladle.

3.2 Temperature Field Analysis of Empty Ladle in Static State

Similarly, taking the temperature distribution of the lining in the stable state as the initial condition, the temperature of the ladle in the static state of the empty ladle is studied. After natural cooling for 2h, the cloud diagram of the temperature distribution of the ladle section in the empty ladle state is shown in Figure 12.

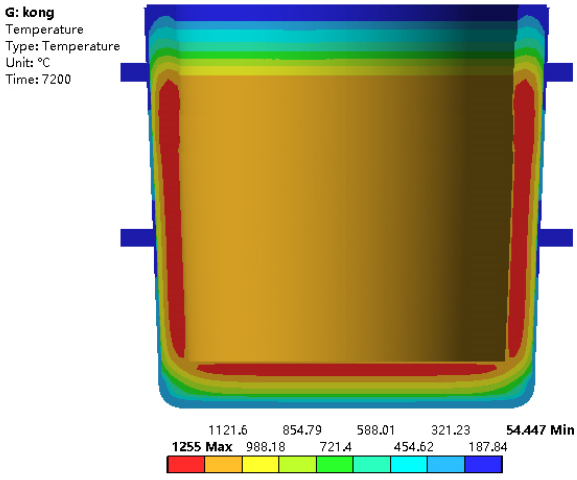

Fig. 12 Temperature distribution of ladle cross-section after empty ladle rest for 2 hours

The temperature distribution of each refractory layer in this state is shown in Table 5.

Table 5 Temperature distribution of refractory layer

Layer	*Average temperature* (℃)	*Maximum temperature* (℃)	*Minimum temperature* (℃)
Working layer	1065	1255	373
Slag line layer	972	1246	317
Permanent layer	754	1183	142
Nano thermal insulation layer	461	903	100
Shell	149	280	54

The temperature distribution of each inner lining layer of the ladle in this state is shown in Figure 13.

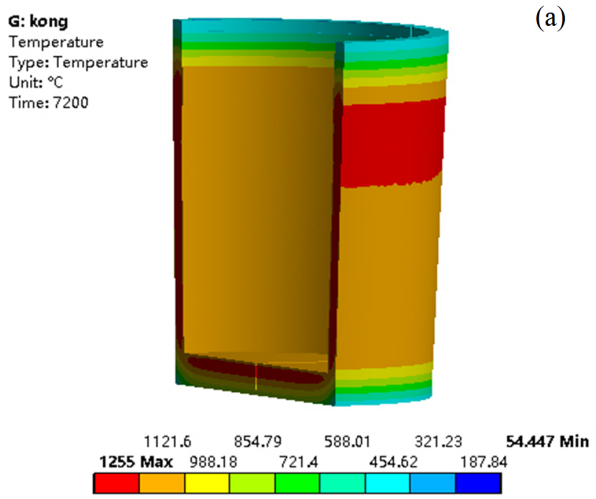

(a) Working layer

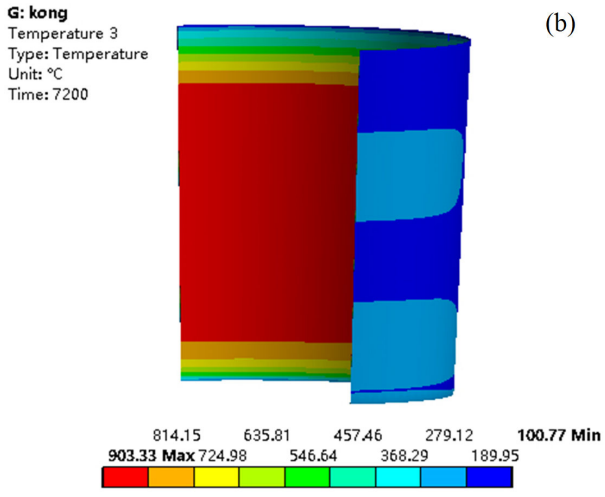

(b) Nano thermal insulation layer

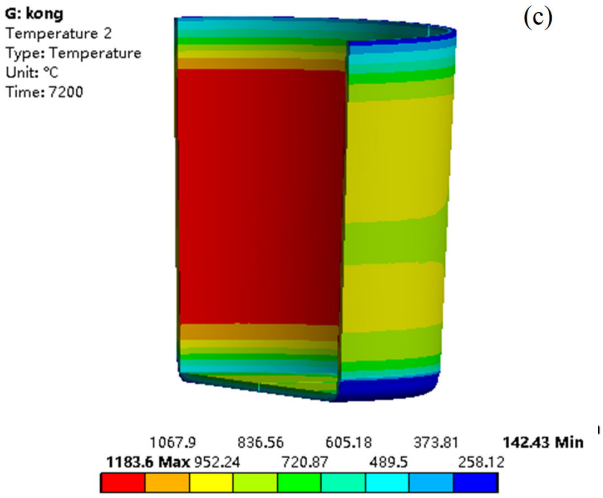

(c) Permanent layer

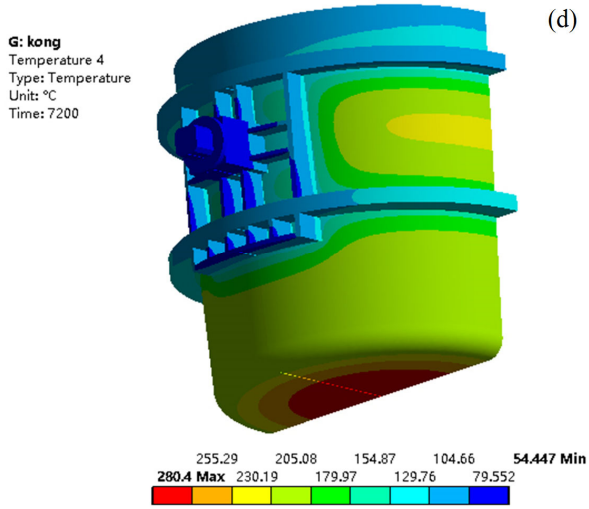

(d) Ladle shell

Fig. 13 Temperature distribution of each inner lining layer of the ladle in the static state of empty ladle

According to the analysis results, the temperature changes of the working layer and slag line layer along the thickness direction after the empty ladle stands for 2h are shown in Figure 14. In this state, the average temperatures of these two parts are about 1065℃ and 972℃ respectively, which is significantly lower than that in the heavy ladle state. The working layer is reduced by 90℃ and the slag line layer is reduced by 111℃; Moreover, the temperature change trend along the thickness direction has also changed, and the temperature no longer shows a trend of high inside and low outside with linear reduction. This is because the ladle lining lacks high-temperature molten steel as a stable heat source in the empty ladle state, and the lining will convective and radiant heat exchange with the outside air, resulting in the rapid reduction of the temperature at the high-temperature part on the inner side, while the nano thermal insulation layer is used as the thermal insulation layer on the outer side, the temperature change is not as severe as the part in contact with the air inside, so the temperature outside is higher than that inside at this time.

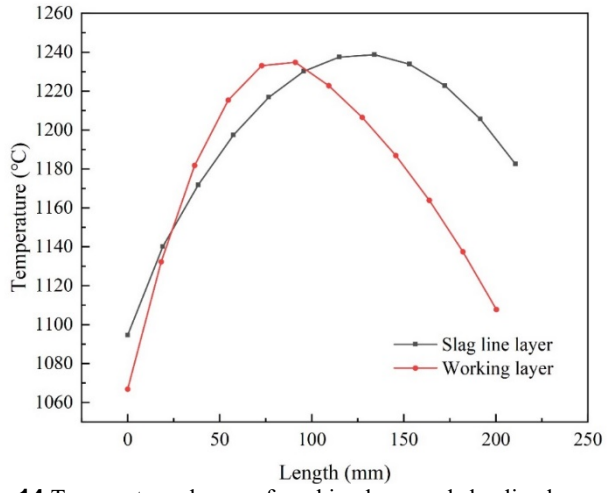

Fig. 14 Temperature change of working layer and slag line layer wall in thickness direction

The temperature change of the permanent layer along the thickness direction is shown in Figure 15. In this state, the average temperature of the permanent layer is maintained at about 754 ℃, and the maximum temperature is 1183 ℃, which is 10 ℃ lower than that in the static state of heavy ladle, and the temperature distribution has not changed significantly.

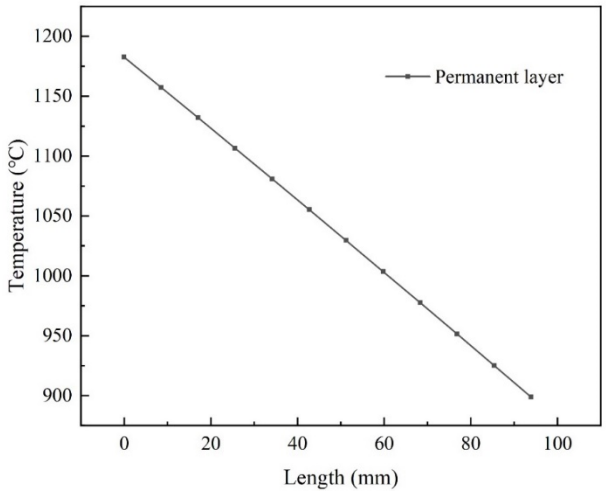

Fig. 15 Temperature change in the thickness direction of the permanent layer

The temperature change of the nano thermal insulation layer along the thickness direction is shown in Figure 16. The average temperature of the layer changes little compared with that in the static state of the heavy ladle, which is about 461℃. The overall temperature distribution is almost the same as that in the steel filled state. Large temperature gradients are still maintained between the inner and outer sides of the nano thermal insulation layer.

The temperature change of the inner and outer walls of the ladle shell in the direction of the axis is shown in Figure 17. The overall temperature distribution and temperature change of the ladle shell are not significantly different from that of the steel filled state. The overall temperature on the inner side of the ladle shell is slightly higher than that on the outer side. The maximum temperature is also about 280 ℃, which appears at the bottom of the ladle, and the minimum temperature appears at the trunnion of the ladle.

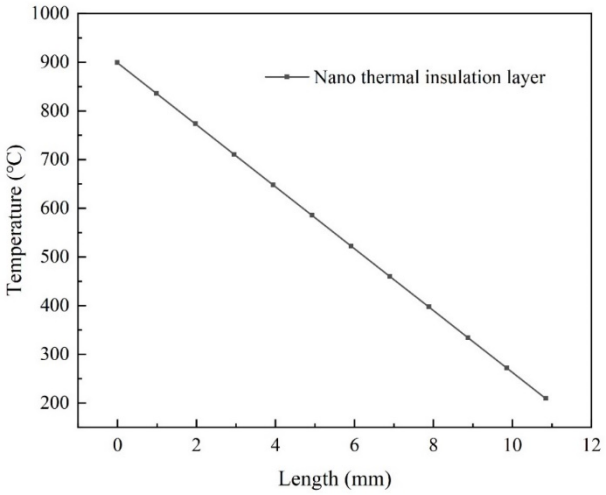

Fig. 16 Temperature change in the thickness direction of the Nano thermal insulation layer

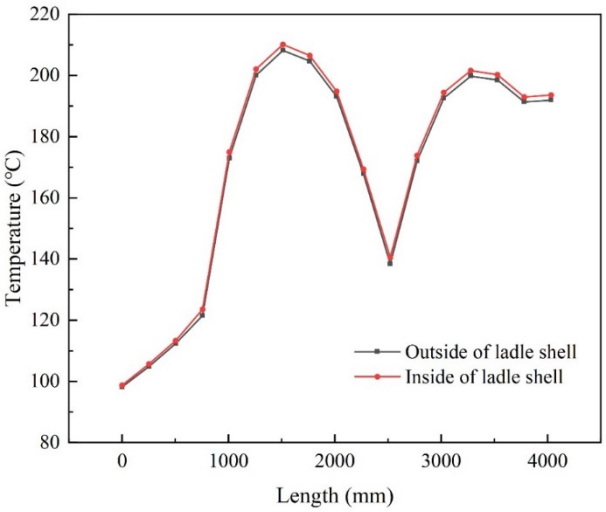

Fig. 17 Temperature change of inner and outer walls of ladle shell in axial direction

Through comparative analysis, compared with the heavy ladle state, due to the lack of high-temperature molten steel as the heat source in the empty ladle state, the temperatures of the working layer and permanent layer are significantly reduced after natural cooling for a period of time, and the temperature change trend of the working layer and slag line layer along the thickness direction is changed due to the change of boundary conditions; Owing to the good thermal insulation performance of the nano thermal insulation layer, the temperature difference between the thermal insulation layer and the ladle shell is small compared with the heavy ladle state.

4. CONCLUSIONS

The ladle with nano thermal insulation material has excellent thermal insulation performance, and the temperature difference between the inner and outer surfaces of the nano thermal insulation layer reaches 696 ° C in the heavy ladle state, which verifies the thermal insulation performance of the nano thermal insulation layer and shows that it can reduce the heat loss of the ladle to a large extent.

Compared with the heavy ladle state, in the empty ladle state, due to the lack of high-temperature heat source, the temperature drop rate of the working layer and slag line layer is significantly higher. The high temperature gradient is an important reason for the damage of the lining refractory material. Therefore, in the production process, the empty ladle time should be reduced as much as possible, or measures such as ladle capping should be taken to avoid sharp temperature changes.

Under the condition of heavy ladle and empty ladle, the temperature distribution of the lining generally shows a trend of high inside and low outside. There is a large temperature gradient along the radial direction, which is easy to cause material damage. Therefore, it is necessary to maintain the lining regularly.

ACKNOWLEDGEMENTS

This research was fully funded by the National Key R&D Program (No. 2018YFB0605900).

NOMENCLATURE

C_p	Specific heat capacity(J/kg·k)
f_x	Mass power along the directions x(m/s^2)
f_y	Mass power along the directions y(m/s^2)
f_z	Mass power along the directions z(m/s^2)
p	Liquid pressure (Pa)
S_T	Source item
S_h	Heat source
t	Time(s)
T	Temperature(K)
v_x	Velocity along the directions of x(m/s)
v_y	Velocity along the directions of y(m/s)
v_z	Velocity along the directions of z(m/s)

Greek Symbols

ρ	Fluid density(kg/m^3)
υ	Kinematic viscosity of fluid(m^2/s)
λ	Thermal conductivity of fluid(W/(m·K))
Φ	Dissipation function

REFERENCES

Kang, J. F., Zhao, M. M., Jiang, Y. C., and Rui, J., 2014, "Research on the Relationship between Restraint Degree and Temperature Stress," *Journal of Water Resources and Architectural Engineering*, 21-25. https://doi.org/10.3969/j.issn.1672-1144.2014.06.004.

Wu, X. H., Meng, X. W., Chen, L., and Zheng, C. L., 2018, "Numerical Simulation of Ladle Temperature Field under Ladle Baking and Steel Filling Conditions," *Electronics Quality*, 84-89. https://doi.org/10.3969/j.issn.1003-0107.2018.07.024.

Liu, Y., 2017, "Simulation on Thermal-mechanical Integrated Stress of Ladle," *Heavy Machinery*, 31-34. https://doi.org/10.13551/j.cnki.zxjxqk.2017.05.007.

Kondrukevich, A. A., and Ryabyi, D. V., 2018, "Effect of Operational Factors on Steel-Teeming Ladle Lining Working Layer Life," *Refractories and Industrial Ceramics*, 58(5), 469-474. https://doi.org/10.1007/s11148-018-0129-0.

Schmitt, N., Berthaud, Y., Hernandez, J. F., Meunier, P., and Poirier, J., 2004, "Damage of Monolithic Refractory Linings in Steel Ladles During Drying," *British Ceramic Transactions*, 103(3), 121-133. https://doi.org/10.1179/096797804225012873.

Ning, L., Xie, Y., and Ma, R., 2019, "Fatigue Analysis of Ladle Shell and Prediction of Lining Thickness," *IOP Conference Series: Materials Science and Engineering*, 631(2), 022031. https://doi.org/10.1088/1757-899X/631/2/022031.

Global Digital Central
ISSN: 2151-8629

Ryabyi, D. V., Kondrukevich, A. A., and Semiryagin, S. V., 2017, "Steel-Pouring Ladle Periclase-Carbon Lining Local (Pitting) Wear Formation Mechanism," *Refractories and Industrial Ceramics*, 57(5), 435-438. https://doi.org/10.1007/s11148-017-9999-9.

Gruber, D., and Harmuth, H., 2014, "Thermomechanical Behavior of Steel Ladle Linings and the Influence of Insulations," *Steel Research International*, 85(4), 512-518. https://doi.org/10.1002/srin.201300129.

Wahlquist, S., Ali, A., Yoon, S. J., and Sabharwall, P., 2022, "Laminar Flow Heat Transfer in Helical Oval-Twisted Tube for Heat Exchanger Applications," *Frontiers in Heat and Mass Transfer*, 18. http://dx.doi.org/10.5098/hmt.18.35.

Prasad, R. S., Singh, S. N., and Gupta, A. K., 2022, "Numerical Investigation of Coupled Natural Convection and Surface Radiation in a Square Cavity with the Linearly Heated Side Wall(s)," *Frontiers in Heat and Mass Transfer*, 19. http://dx.doi.org/10.5098/hmt.19.16.

Zabolotsky, A. V., 2011, "Modeling of the Temperature Field of the Casting Ladle Lining," *Journal of Engineering Physics and Thermophysics*, 84(2), 342-347. https://doi.org/10.1007/s10891-011-0478-8.

Volkova, O., and Janke, D., 2003, "Modelling of Temperature Distribution in Refractory Ladle Lining for Steelmaking," *ISIJ International*, 43(8), 1185-1190. https://doi.org/10.2355/isijinternational.43.1185.

Cheng, B. J., Li, P. F., Tan, S. Q., and Zhao, Q. C., 2015, "Influence of Preheating Temperature on Lining Temperature and Stress when Ladle is Filled with Steel," *Journal of Iron and Steel Research*, 27(9), 39-43. https://doi.org/10.13228/j.boyuan.issn1001-0963.20140210.

Li, G. F., Liu, J., Jiang, G. Z., and Liu, H. H., 2015, "Numerical Simulation of Temperature Field and Thermal Stress Field in the New Type of Ladle with the Nanometer Adiabatic Material," *Advances in Mechanical Engineering*, 1687814015575988. https://doi.org/10.1177/1687814015575988.

Farrera-Buenrostro, J. E., Hernandez-Bocanegra, C. A., Ramos-Banderas, J.A., Torres-Alonso, E., Lopez-Granados, N.M., and Ramirez-Argaez, M.A., 2019, "Analysis of Temperature Losses of the Liquid Steel in a Ladle Furnace During Desulfurization Stage," *Transactions of the Indian Institute of Metals*, 72(4), 899-909. https://doi.org/10.1007/s12666-018-1548-9.

Sun, Y., Tian, J. R., Du, J., Bo, T., Liu, Y., Yun, J. T., and Chen, D. S., 2020, "Numerical Simulation Thermal Insulation and Longevity Performance in New Lightweight Ladle," *Concurrency and Computation Practice and Experience*, 32(22), 5830. https://doi.org/10.1002/cpe.5830.

Qiu, H., Han, W. G., Liu, H. P., and Sha, Y. Y., 2022, "Numerical Simulation of Hot Metal Temperature Drop during Holding Period in 210t Ladle," *Journal of Iron and Steel Research*, 34(2022), 212-221. https://doi.org/10.13228/j.boyuan.issn1001-0963.20210116.

Bhagat, R. D. and Deshmukh, S. J., 2021, "Numerical Analysis of Passive Two Phase Fluid Flow in a Closed Loop Pulsating Heat Pipe," *Frontiers in Heat and Mass Transfer*, 16. http://dx.doi.org/10.5098/hmt.16.23.